Accepted Manuscript

Synthesis and biological evaluation of a Platinum(II)-c(RGDyK) conjugate for integrin-targeted photodynamic therapy

T. Chatzisideri, S. Thysiadis, S. Katsamakas, P. Dalezis, I. Sigala, T. Lazarides, E. Nikolakaki, D. Trafalis, O.A. Gederaas, M. Lindgren, V. Sarli

PII: S0223-5234(17)30773-0

DOI: 10.1016/j.ejmech.2017.09.058

Reference: EJMECH 9773

To appear in: *European Journal of Medicinal Chemistry*

Received Date: 20 June 2017

Revised Date: 25 September 2017

Accepted Date: 27 September 2017

Please cite this article as: T. Chatzisideri, S. Thysiadis, S. Katsamakas, P. Dalezis, I. Sigala, T. Lazarides, E. Nikolakaki, D. Trafalis, O.A. Gederaas, M. Lindgren, V. Sarli, Synthesis and biological evaluation of a Platinum(II)-c(RGDyK) conjugate for integrin-targeted photodynamic therapy, *European Journal of Medicinal Chemistry* (2017), doi: 10.1016/j.ejmech.2017.09.058.

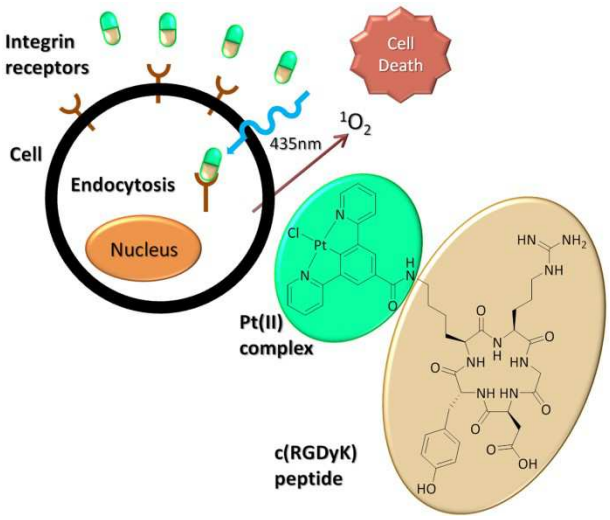

Synthesis and Biological Evaluation of a Platinum(II)-c(RGDyK) Conjugate for Integrin-Targeted Photodynamic Therapy

T. Chatzisideri,[a] S. Thysiadis,[a] S. Katsamakas,[b] P. Dalezis,[c] I. Sigala,[a] T. Lazarides,[a] E. Nikolakaki,[a] D. Trafalis,[c] O. A. Gederaas,[d] M. Lindgren[e] and V. Sarli*,[a]

[a] Department of Chemistry, Aristotle University of Thessaloniki, University Campus, 54124, Thessaloniki, Greece, sarli@chem.auth.gr

[b] Department of Pharmaceutical Chemistry, School of Pharmacy, Aristotle University of Thessaloniki, University Campus, 54124, Thessaloniki, Greece

[c] Laboratory of Pharmacology, Medical School National and Kapodistrian University of Athens 75 Mikras Asias Street, Athens, 11527, Greece, dtrafal@med.uoa.gr

[d] Department of Cancer Research and Molecular Medicine, Norwegian University of Science and Technology, NTNU, N-7491 Trondheim, Norway, odrun.gederaas@ntnu.no

[e] Department of Physics, Norwegian University of Science and Technology, NTNU, N-7491 Trondheim, Norway, mikael.lindgren@ntnu.no

Highlights

- A cancer-targeting conjugate of a cyclometalated [N,C,N-Pt(II)] complex has been synthesised
- The conjugate exhibited a mild cytostatic effect to six different cancer cell lines
- The conjugate demonstrated rapid cell uptake by receptor-mediated endocytosis
- The conjugate efficiently generated $^1O_2$ upon irradiation
- Conjugate **4** resulted in reduction of cell survival of AY27 cells after blue light exposure

Abstract

A cancer-targeting conjugate **4** of a cyclometalated [N,C,N-Pt(II)] complex bearing a N^C^N 1,3-di(2-pyridyl)-benzene with c(RGDyK) peptide as guiding molecule was designed and synthesized for real-time drug delivery monitoring in cancer cells and photodynamic therapy (PDT). This conjugate demonstrates a mild cytostatic effect to six cancer cell lines expressing integrins at different extent, while possessing promising

features for PDT. Conjugate **4** demonstrated rapid cell uptake by receptor-mediated endocytosis and efficient generation of $^1O_2$ upon irradiation. Incubation of rat bladder cancer cells AY27 with conjugate **4** (50 μM) prior to blue light exposure (5 min) resulted in significant reduction (50%) of cell survival compared to control cells as measured by MTT assay post 24 h after treatment.

Keywords: Targeted drug delivery, RGD peptide, integrin avβ3, Angiogenesis, Tumor therapy, Pt(II)-RGD conjugate, Photodynamic therapy, theranostic agent

Introduction

Photodynamic therapy (PDT) is a clinically approved method in oncology, by which photosensitizers (PSs) generate cytotoxic reactive oxygen species (ROS) for the efficient killing of cancer cells under visible light illumination via oxidative damage [1]. PDT has been applied for the treatment of various cancers such as melanoma, head and neck, bladder, breast, and pulmonary carcinomas [2,3,4,5]. Main factors that determine PDT efficacy include the PS's ability to produce ROS, as well as its selectivity and targeting ability [6]. Presently, scientific endeavors have focused on the development of targeted drug delivery systems for effective delivery of PSs [7].

Targeted drug delivery offers an attractive strategy to achieve the most of the drug's potential therapeutic benefit and minimize any undesirable side effects at the lowest dose [8,9]. Peptides such as Arg-Gly-Asp (RGD) peptides [10,11], octreotide [12], bombesin [13] and poly-Arg peptides [14] have been extensively used as carriers to selectively direct drugs to cancer cells with upregulated receptors [15, 16]. A variety of linear as well as cyclic RGD peptide delivery systems with cytotoxic drugs have been developed to target integrin receptors $\alpha_v\beta_3$ and $\alpha_v\beta_5$ that are overexpressed in several cancer types such as melanoma, glioblastoma, ovarian, prostate and breast cancer [17, 18, 19, 20, 21]. RGD conjugates for theranostic applications are also available for monitoring of drug release to ensure efficient delivery [22]. Commonly employed labels that allow effective drug monitoring by the use of various fluorescence microscopy techniques include luminescent complexes of transition metals [23,24]. These complexes have been proved effective for live cell imaging and *in vivo* detection of target molecules [25].

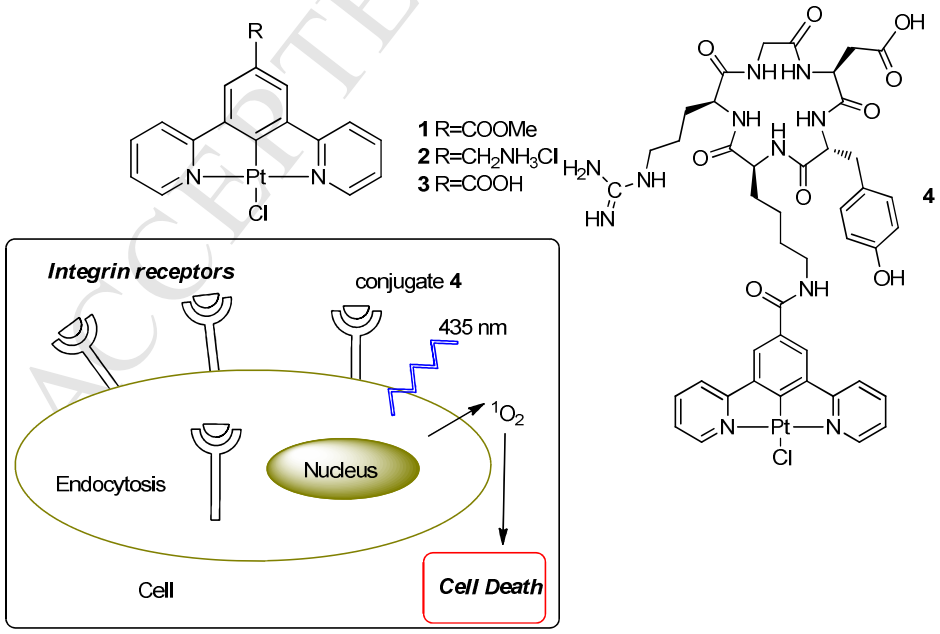

Scheme 1. Schematic illustration of [N,C,N-Pt(II)]-c(RGDyK) conjugate **4** for integrin-targeted PDT

In particular, cyclometalated Pt(II) complexes display useful photochemical properties and have been extensively studied for their use as agents for biological labeling [26], chemosensors [27], phosphorescent emitters in organic light-emitting diodes (OLEDs) [28], photocatalysts [29], anticancer agents [30], optical power limiting [31] and photovoltaic devices [32]. Another important application of platinum (II) complexes is in cancer chemotherapy [33]. Cisplatin, carboplatin, and oxaliplatin are among the most widely used antitumor agents. However, their clinical application is limited by acquired or intrinsic resistance and/or their high toxicity mainly due to their nonselective mode of action [34]. Platinum complexes exhibit cytostatic effects by interacting with DNA, thus inhibiting the DNA synthesis.

In this study, we aimed to develop a novel delivery system of a Pt(II) complex with c(RGDyK) peptide suitable for targeted tumor therapy and theragnostic applications. Toward this direction, [N,C,N-Pt(II)] complex **3** was attached to c(RGDyK) via a stable amide bond. Complex **3** bearing a N^C^N 1,3-di(2-pyridyl)-benzene was employed based on its reported advantageous photophysical and antiproliferative properties (Scheme 1). De Cola and coworkers have previously reported the activities of a series of [N,C,N-Pt(II)] complexes as well as their application as bio-imaging probes [35]. They have shown that these complexes display wide emission color tunability, a very large Stokes shift and long lived luminescent excited states. In another study, the water soluble, cyclometalated [N,C,N-Pt(II)] complex **2** has been used for imaging of live cells and histological tissues with high resolution by "two-photon time-resolved emission imaging microscopy" (TP-TREM) [36]. In addition, Weinstein and Bryant showed that complex **1** induces photodynamic killing in a range of cancer cells including a cisplatin resistant cell line [37]. Herein, we show that the [N,C,N-Pt(II)]-c(RGDyK) conjugate **4** exhibits a moderate cytostatic activity in a panel of integrin expressing cancer cells *in vitro* and possesses promising photochemical properties for PDT applications in rat bladder cancer cells (AY27).

Results and discussion

Synthesis of [N,C,N-Pt(II)]-c(RGDyK) conjugate 4

The synthesis of conjugate **4** is outlined in Scheme 2. Methyl 3,5-dibromobenzoate **5** was subjected to reaction with pinacolborane in the presence of $Pd(dppf)Cl_2$ under microwave irradiation to give aryl boronic ester **6** [38]. A Suzuki–Miyaura coupling of **6** with 2-chloropyridine using $Pd(OAc)_2$, PPh_3 and Na_2CO_3 in THF and H_2O at 85 °C yielded methyl 3,5-di(pyridin-2-yl)benzoate in 63% yield. Cycloplatination with K_2PtCl_4 in CH_3CN as previously described [39], followed by methyl ester hydrolysis afforded the desired acid **3** [40]. Subsequently, [N,C,N-Pt(II)] complex **3** was activated using EDCI and NHS and the resulting *N*-hydroxysuccinimidyl ester was coupled with the c(RGDyK) peptide lysine amino group to give conjugate **4** in excellent yield. The cycloplatinated structures of **3** and **4** were confirmed by ^{1}H-NMR and mass spectrometry (ESI-MS for $C_{44}H_{51}ClN_{11}O_9Pt^+$ $[M+H]^+$=1107.32, was found 1107.95, Figure S2).

After HPLC purification of **4**, ESI-LCMS analysis revealed that the purity of **4** was greater than 93%. When the same sample after HPLC purification was lyophilized, dissolved in MeOH/DMF and analyzed again, one more peak was observed in the chromatograph, which was attributed probably to platinum(II) aqua complex **7**. When this product was isolated by HPLC and analyzed again the chromatograph indicated the presence of **4**. Thus, it seems that the two compounds are in equilibrium and interconvert under certain conditions possibly as a consequence of reversible ligand exchange reactions. The molecular ions at *m/z* 556, 1071, 1186 were interpreted as $[M\text{-}Cl+H+CH_3CN]^{2+}/2$, $[M\text{-}Cl]^+$, $[M+H+2CH_3CN]^+$ species (Figure S2). A number of experiments were performed involving the ionization of **4** with or without chromatographic separation diluted in different solvents. The study of the hydrolysis of **4** by the LC-MS method was very challenging, as the intermediate platinum(II) aqua complexes were highly reactive with organic molecules, solvents and ions and the complexes observed via ESI-MS did not always match with the species in solution (Figure S2, S3 S4). For example the peak at *m/z* 1097.75 was attributed to $[M\text{-}Cl+N_2]^+$ arising from the clustering of $[M\text{-}Cl]^+$ with dissolvation gas, a phenomenon previously observed during the ESI-MS ionization of cis-platin [41]. It should also be noted that **4** displays poor solubility in water and it was dissolved in DMSO prior to biological experiments.

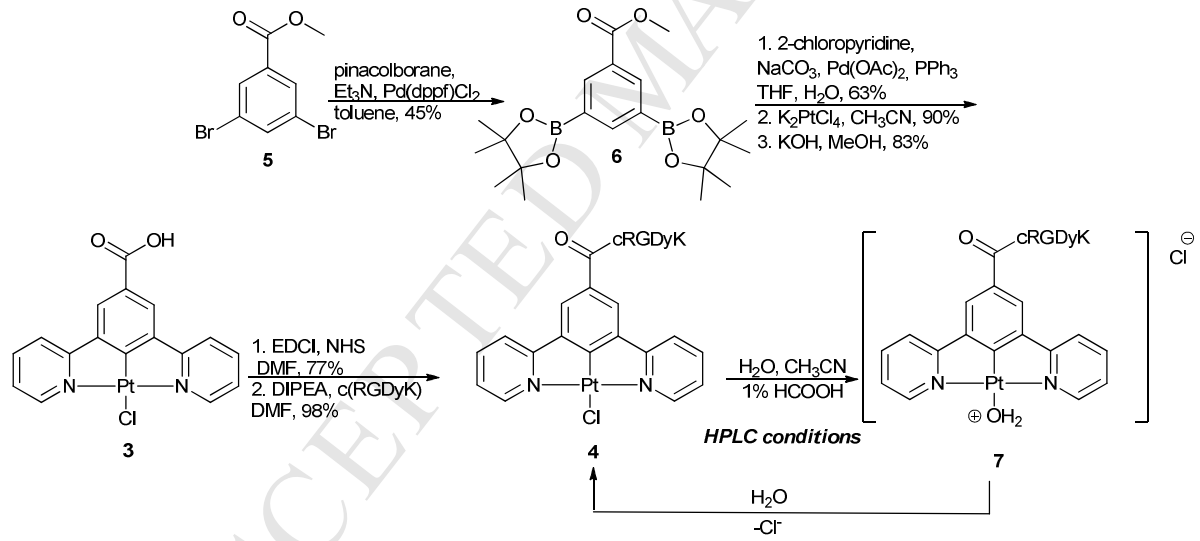

Scheme 2. Synthesis of [N,C,N-Pt(II)]-c(RGDyK) conjugate **4**

The UV-vis absorption spectrum of conjugate **4** in DMSO solution is dominated by strong absorption bands in the UV region (λ < 300 nm), which are attributed to $^1\pi$-π^* transitions of the ligand and the phenol moiety of tyrosine. The lowest energy absorption band of conjugate **4** lies in the region between 350 and 440 nm and is attributed to overlapping ligand based $^1\pi$-π^* and singlet metal-to-ligand-charge-transfer transitions (^{1}MLCT) [39]. Selective excitation of the platinum chromophore of conjugate **4** at 400 nm, gives rise to a structured emission band with maximum at ca. 487 nm attributed to a transition of predominantly ligand

based $^3\pi$-π^* character [39]. The good match between the absorption and excitation profiles further confirms that the emission of conjugate **4** originates from the platinum(II) chromophore. These spectroscopic observations are in excellent agreement with those made in the cases of similar platinum(II) complexes [39] indicating that the cyclometallated chromophore is virtually unaffected by conjugation to the peptide. It is worth noting that in more concentrated solutions (>5 × 10^{-6} M) in aqueous solvent mixtures, the emission spectra of **4** are dominated by a featureless excimer band centred at ca. 660 nm (Figure S2) indicating that even in the presence of the bulky peptide moiety, the platinum chromophores are still able to stack and form excimers under certain conditions.

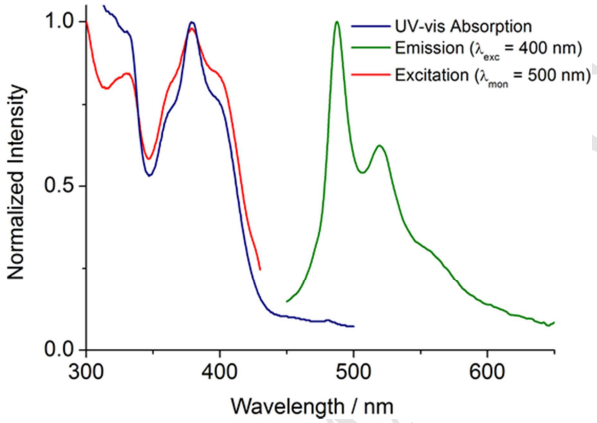

Figure 1: Normalized absorption, emission and excitation profiles of conjugate **4** in DMSO solution (5 × 10^{-6} M).

Reactivity of [N,C,N-Pt(II)]-c(RGDyK) conjugate 4 toward amino acids and water

In order to study the behavior of conjugate **4** in a biological system, the reactivity of model complex **3** in aqueous solution was also investigated. The hydrolysis and the reversibility of the hydrolysis of **3** were studied by analyzing the ^{1}H-NMR spectra of (~8.5 mM) solutions of **3** in d_6-DMSO/D_2O (9/1 v/v) at 25 °C, both without NaCl and in the presence of 10 mM NaCl. The ^{1}H NMR spectra of complex **3** (~8.5 mM) in d_6-DMSO, and in d_6-DMSO/D_2O (9/1 v/v) are shown in Figure 2A and Figure 2B, indicating the fast hydrolysis of **3** after 10 min in the aqueous medium. The reversibility of the hydrolysis in the presence of NaCl (10 mM) is shown in Figure 2C indicating that the hydrolyzed sample of **3** most probably returns quantitatively to the chlorido complex. In addition, the ESI-MS data of **3** (dissolved in DMSO/H_2O=9/1) revealed a set of peaks at m/z 510.65 showing the Pt isotope pattern, which is attributed to hydroxido platinum(II) complex [M-Cl+OH+Na]$^+$ (Figure S7).

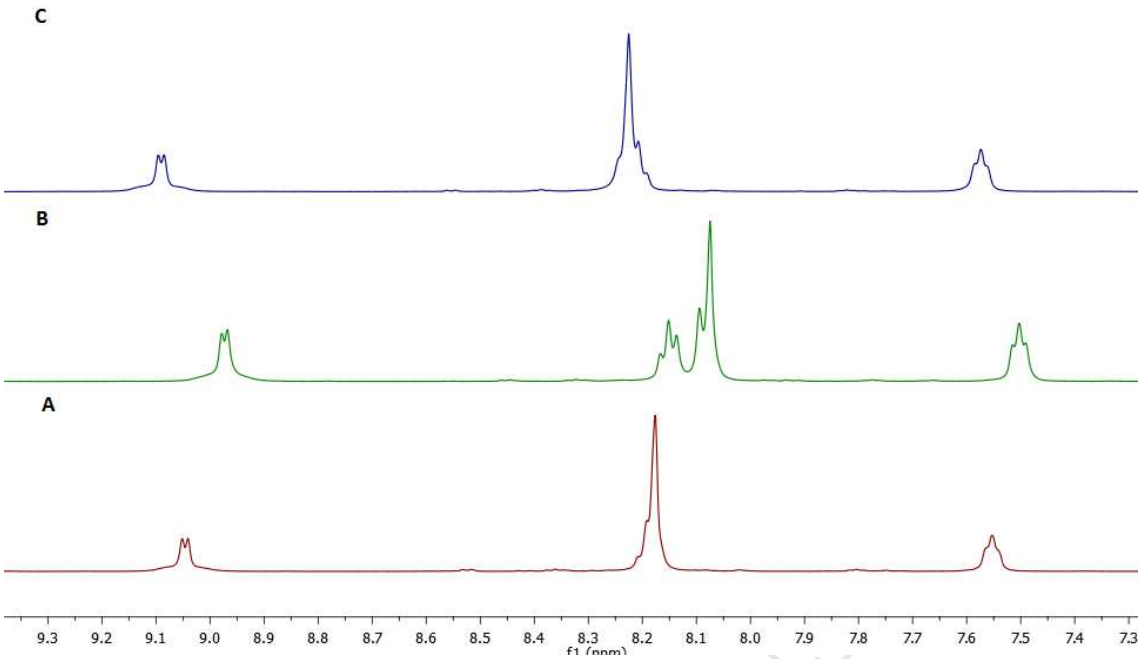

Figure 2. ^{1}H NMR (500 MHz) spectra of complex **3** in (A) d_6-DMSO and (B) d_6-DMSO (90%) /D_2O (10%) after 10 min. C) Addition of NaCl 10 mM to sample of (B) after 30 min.

To evaluate the stability of conjugate **4** at different pH values, it was dissolved in DMSO/MeOH and diluted with phosphate or acetate buffers at 37 °C. The LC-MS analysis data indicated the hydrolysis of **4** after 24h at both physiological pH 7.4 buffer and acidic pH 5.2 (Figure S8, S9). The reactivity of conjugate **4** toward small biomolecules was also assessed by studying the reaction of **4** with selected amino acids such as L-histidine (His), L-cysteine (Cys), and glycine (Gly). Conjugate **4** was incubated with an equimolar mixture of Gly, Cys, and His and the reaction mixture was analyzed by ESI-LCMS. After 6 h, amino acid adduct peaks started to form preferably with Cys $[(M\text{-}Cl+2Cys+2H)^{2+}]/2=656$ and His $[(M\text{-}Cl+His+2Na)^{2+}/2= 636]$. It should be noted that precipitation of insoluble platinum compounds were largely observed.

Photosensitising properties of [N,C,N-Pt(II)]-c(RGDyK) conjugate 4

In order to confirm the production of singlet oxygen, triplet excited state absorption recorded for UV excitation (λ = 355 nm, Figure 3A) and the subsequent formation of singlet oxygen, was measured from the direct luminescence at 1275 nm (Figure 3B). Firstly, solutions of compounds **3** and **4** in DMSO with the same concentration corresponding to an absorbance of approximately 0.15, were prepared (Figure 3C). In order to prove the existence of triplet states in **3** and **4**, excited state absorption was measured by exciting Argon flushed samples with ns laser pulse at 355 nm, and recording the full spectrum with a broad band flash lamp and a gated detector synchronized with the excitation pulse. These spectra (Figure 3A) show depleted absorption bands in the 350 -420 nm region due to bleaching of the ground states of **3** and **4** (view

comparison with ground state absorption spectra in Figure 3C) accompanied by the emergence of broad low-energy absorption signals in the 400-500 nm region. The latter are attributed to ligand-based $^3\pi$-π^* absorptions [42]. Repeating the procedure for a sample containing oxygen the triplet absorption signal are strongly quenched and diminishes (data not shown). Next, the transient singlet oxygen luminescence was verified by exciting the sample using a 420 nm laser and recording the transient luminescence at 1275 nm. Here, an oxygen containing sample was used, and the background subtraction was carried out using the Argon flushed sample for each case. A weak transient signal was observed in both samples using DMSO as solvent (Figure 3B). Complex **3** (but not **7**) exhibited solubility in THF and it was possible to record a much stronger signal from the singlet oxygen (Figure 3B) to confirm the energy transfer from the triplet state to proximate dissolved oxygen.

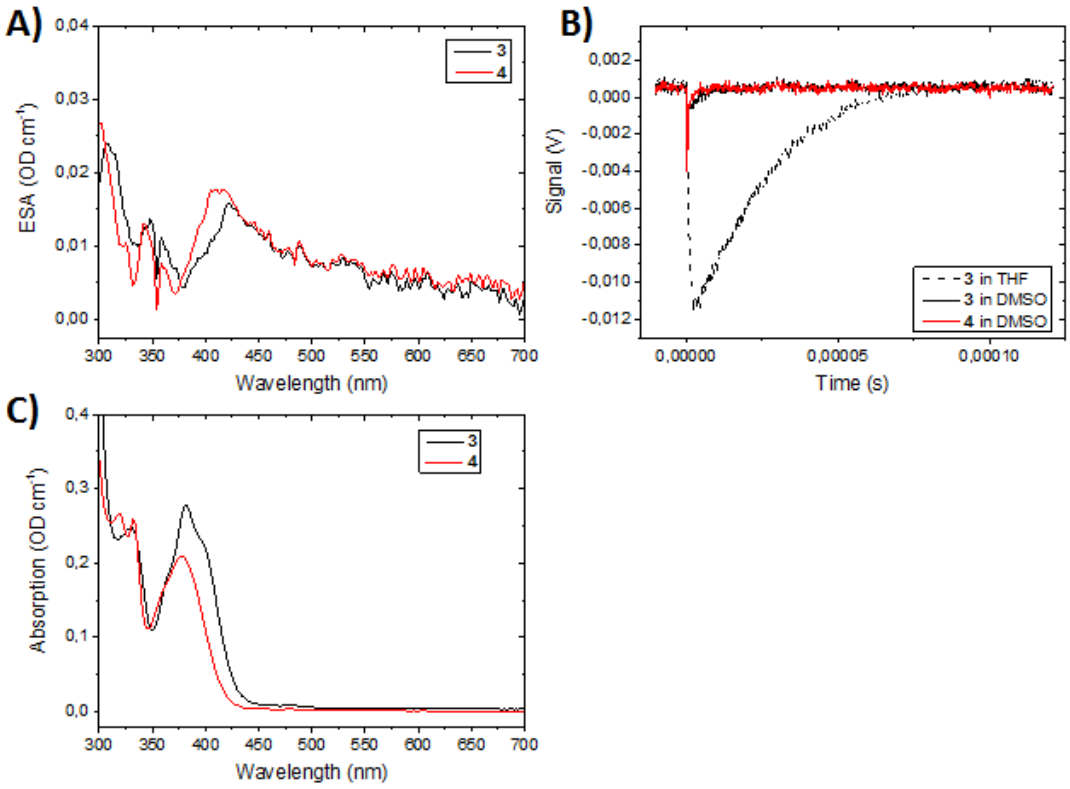

Figure 3. A) Excited state absorption with solutions of **3** and **4** in DMSO, B) Singlet oxygen luminescence at 1275 nm with solutions of **3** and **4** in THF and DMSO, C) Absorption of solutions of **3** and **4** in DMSO used for excited state absorption and singlet oxygen luminescence measurements

Cellular uptake of [N,C,N-Pt(II)]-c(RGDyK) conjugate 4

To demonstrate the role of the RGD moiety in targeting conjugate **4** to $\alpha_v\beta_3$ integrin-rich tumor cells, compounds **3** and **4** were incubated with U87 and Hela cells. The reason for choosing these two cell lines is

because U87 glioblastoma cells contain considerably higher levels of $\alpha_v\beta_3$ integrin receptors than HeLa cells [43, 44, 45, 46]. When U87 cells were treated with **4**, a strong fluorescence signal was observed, indicative of the efficient cellular uptake of conjugate **4**, whereas the fluorescence intensity in HeLa cells was much weaker (Figure 4). The strong fluorescence signal seen in U87 cells is due to $\alpha_v\beta_3$ integrin receptor-mediated endocytosis, since the uptake of an analogous compound **3**, which however lacks an RGD-targeting group, is significantly less.

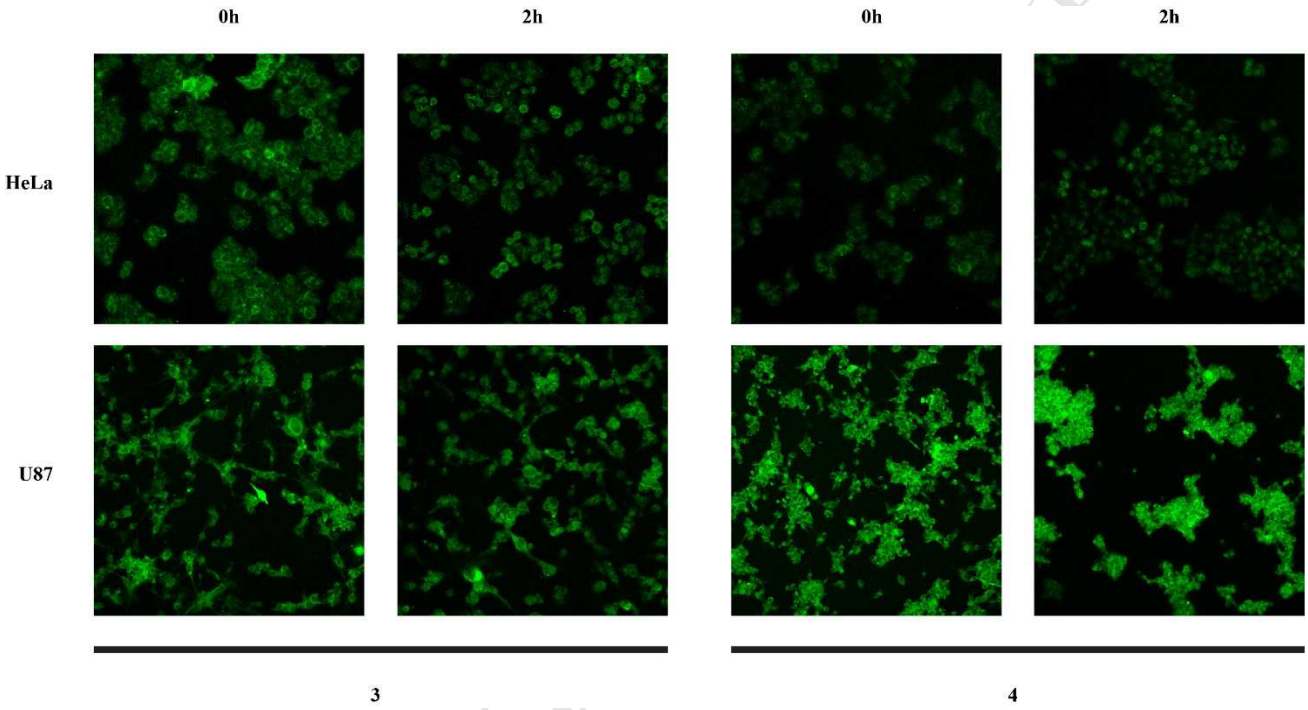

Figure 4. Confocal microscopy images of U87M and HeLa cells after incubation with 10 μM of **4** and **3** for 0 and 2 h, respectively. Cells were then washed twice with PBS to remove floating compounds and were visualized in a Nikon confocal microscope using the EZ-C1 3.20.

To provide further evidence that the uptake of conjugate **4** was mediated through endocytosis, we repeated the experiment using an endocytosis inhibitor, okadaic acid [47, 48, 49]. As it is clearly shown in Figure 5, when U87 cells were treated with **4** the fluorescence signal markedly decreased following addition of 100 nM okadaic acid, whereas, when **3** which lacks the RGD-targeting group was added to U87 cells the fluorescence intensity remained practically unaffected in the presence of okadaic acid.

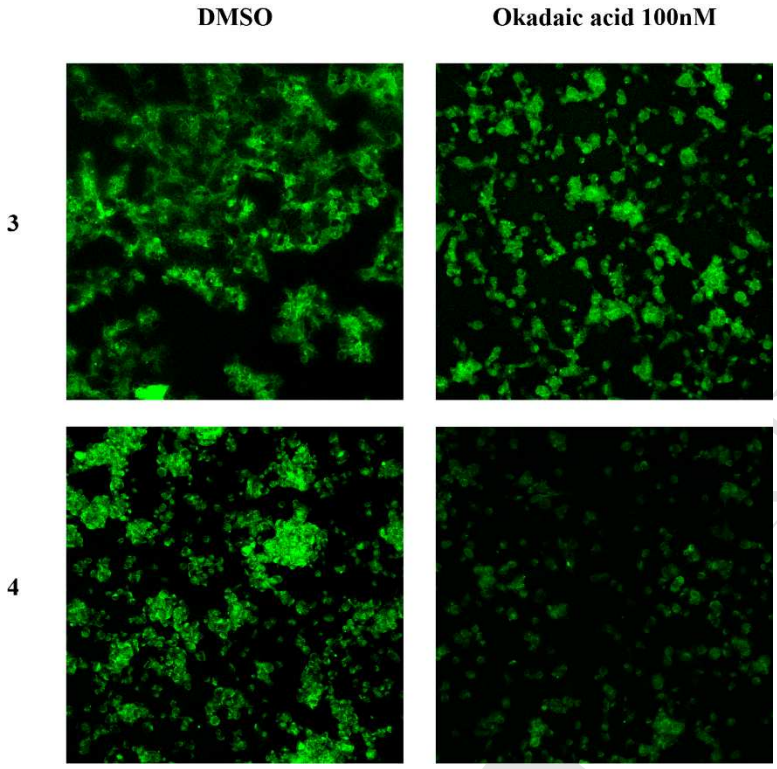

Figure 5. Confocal microscopy images of U87 cells treated with 10 μM of **4** and **3** for 2h. Cells were preincubated, prior to addition of **4** and **3**, with medium containing DMSO (control) or okadaic acid (100 nM) for 30 min. The floating conjugate was removed by washing twice with PBS and cells were then visualized in a Nikon confocal microscope using the EZ-C1 3.20.

Cytotoxicity of [N,C,N-Pt(II)]-c(RGDyK) conjugate 4

The antiproliferative activities of [N,C,N-Pt(II)]-c(RGDyK) conjugate **4** in comparison with c(RGDyK) and complex [N,C,N-Pt(II)] **3** were studied by MTT assays in 6 cell lines of different tumour types. The PC3 [50], SCOV-3 [51], A549 [52], MDA-MB-231 [53,54], MCF-7 cells [55] and U87M [56] cell lines all express integrin $\alpha_v\beta_3$ at different extent. Results regarding the cytostatic and cytotoxic activity of the compound **4** are presented in Table 1. Treatment with c(RGDyK), **3** and **4** reduced the cell growth of all six cell lines at different extent and their IC_{50} values were estimated to be higher than 100 μM. In general, it was demonstrated that the tested compounds exhibit mostly cytostatic activity rather than cytotoxic (Figure 6,7,8). Compounds c(RGDyK), **3** and **4** exhibited a moderate cytostatic effect against PC3 and A549 and a very good cytostatic effect against MDA-MB-231 cell lines. It is worth noting that SKOV-3 are more sensitive to **4** (GI_{50}= 12 μM) than its precursor **3** (GI_{50}>100 μM). The growth inhibitory effect against MDA-MB-231

cells is slightly increased for conjugate **4** GI_{50}= 10 µM, TGI=58 µM versus GI_{50} =26 µM, TGI=78 µM for complex **3**.

Table 1. Growth inhibition/cytostatic (GI_{50} and TGI) and cytotoxic/cytocidal (IC_{50}) anticancer effects induced by c(RGDyK), complex **3** and conjugate **4** on six human cancer cell lines

Cell Lines	c(RGDyK)			Complex 3			Conjugate 7		
	GI_{50}	TGI	IC_{50}	GI_{50}	TGI	IC_{50}	GI_{50}	TGI	IC_{50}
SKOV-3	>100	>100	>100	>100	>100	>100	12	>100	>100
PC-3	74,5	>100	>100	18	49	>100	22	>100	>100
A549	61	>100	>100	28	>100	>100	76	>100	>100
MCF-7	>100	>100	>100	>100	>100	>100	>100	>100	>100
MDA-MB-231	72	>100	>100	26	78	>100	10	58	>100
U87M	40	>100	>100	>100	>100	>100	>100	>100	>100

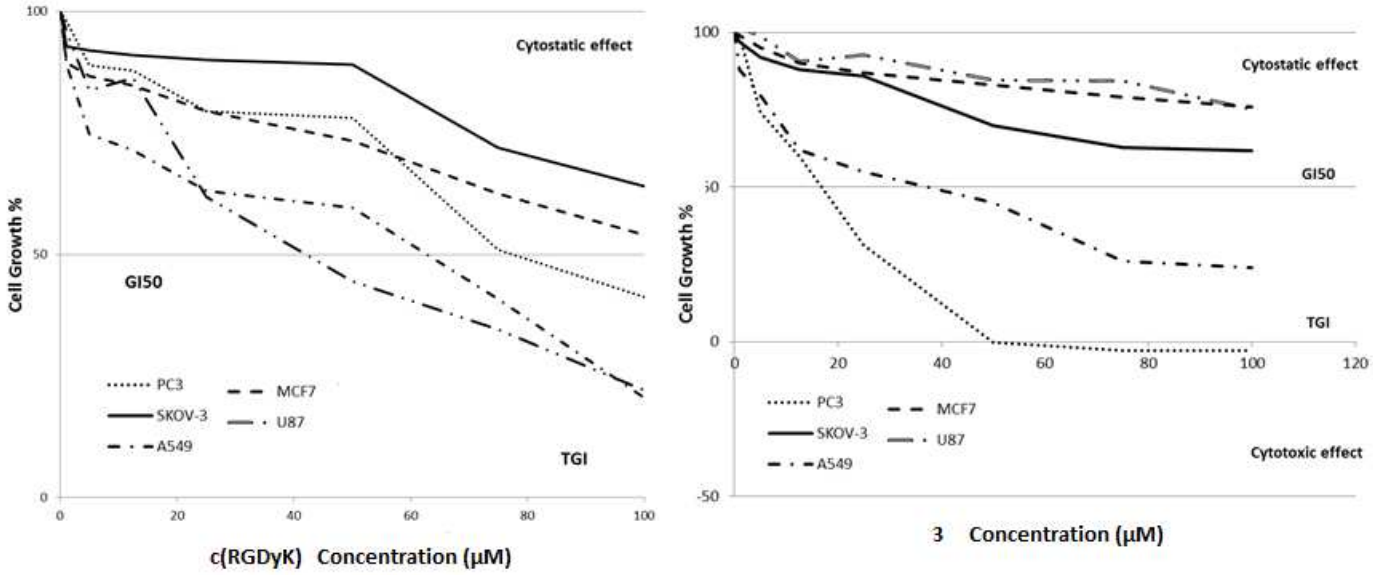

Figure 6. Growth inhibition (sensitivity curves) of PC-3, SKOV-3, A549, MCF7 and U87 cells, produced after treatment with **cRGDyK** and complex **3**. GI_{50} represents the 50% growth inhibition; IC_{50} the half maximal inhibitory concentration and TGI the total growth inhibition.

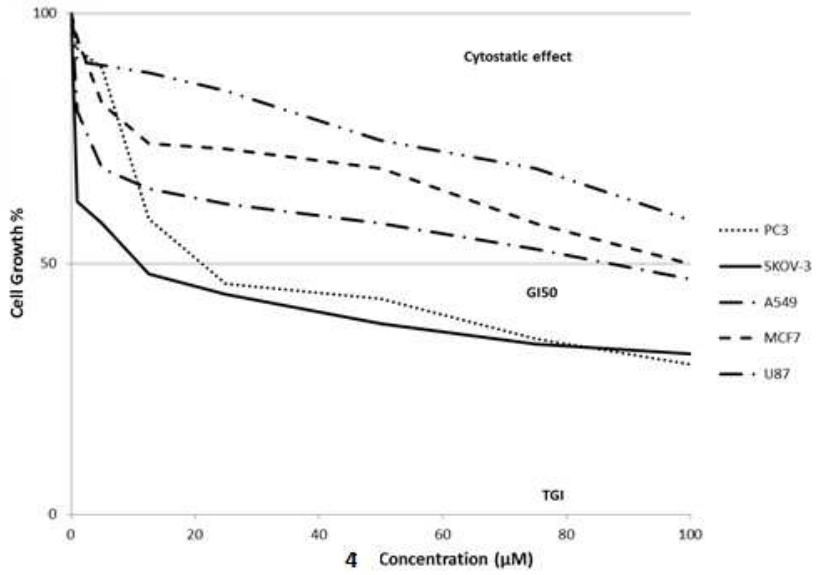

Figure 7. Growth inhibition (sensitivity curves) of PC-3, SKOV-3, A549, MCF7 and U87 cells, produced after treatment with conjugate **4**. GI_{50} represents the 50% growth inhibition; IC_{50} the half maximal inhibitory concentration and TGI the total growth inhibition.

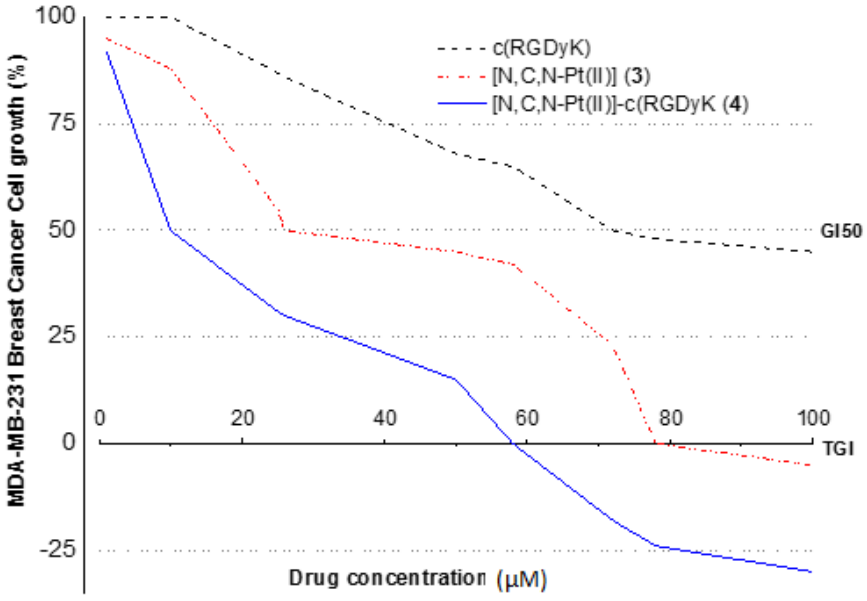

Figure 8. Growth inhibition (sensitivity curves) of MDA-MB-231 cells, produced after treatment with c(RGDyK), complex **3** and conjugate **4**.

To evaluate the potential of conjugate **4** for PDT, the effect of blue light exposure on survival of rat bladder cancer cells (AY27) was determined after treatment with complex **3** and conjugate at different concentrations (Figure 9). This cell line has been previously used in an orthotopic rat bladder cancer model for PDT studies and is chosen to be further applied to *in vivo* experiments [57].

Preliminary PDT experiments show a clear dose dependent reduction of cell viability after blue light exposure. Incubation with conjugate **4** (50 µM) prior to light exposure (5 min) resulted in significant reduction (50%) of cell survival compared to control cells as measured by MTT assay post 24 h after treatment. The experimental data clearly showed cell death in the dark ("dark toxicity") compared to control cells. A reduction of 31% and 43% in cell viability was observed at 0 min of light exposure after treatment with 50 µM of complex **3** and conjugate **4**, respectively. Importantly, it was found that the cell viability effect of **4** is about 10% higher compared to compound **3** (5 min). This finding indicates the important contribution of c(RGDyK) peptide to the anticancer action of conjugate **4**.

Conclusion

Taken together, the results indicate that the combination of complex [N,C,N-Pt(II)] **3** with c(RGDyK) leads to a new delivery system with drug monitoring capabilities and promising anticancer activities for PDT applications. The synthesis, characterization, photophysics, cellular uptake and toxicity after blue light exposure of conjugate **4** has been presented, indicating a great potential of such type of conjugates in targeted photodynamic therapy. Based on these encouraging results, further *in vitro* and *vivo* experiments are in progress and will be reported in due course.

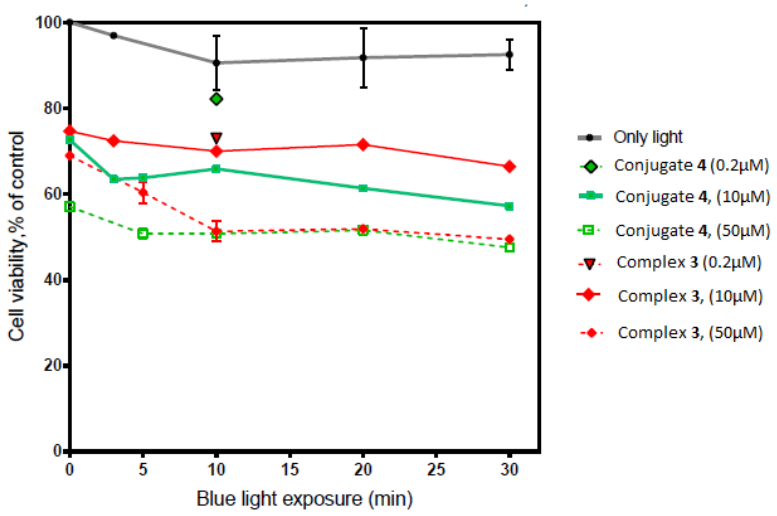

Figure 9. Survival of cancer cells AY27 post 24 h after treatment with complex **3** or conjugate **4**.

Acknowledgements

This programme was implemented within the framework of the IKY/SIEMENS Excellence Research Grants 2016 (Synthesis of anticancer peptide derivatives). S. Katsamakas is thankful to Aristotle University of Thessaloniki Research Committee for financial support through an excellence Post-doctoral Scholarship. The authors declare to have no competing financial interests.

Experimental procedures

General Experimental Details. All reactions were carried out under an atmosphere of Ar unless otherwise specified. Commercial reagents of high purity were purchased and used without further purification, unless otherwise noted. Reactions were monitored by TLC and using UV light as a visualizing agent and aqueous ceric sulfate/phosphomolybdic acid, ethanolic p-anisaldehyde solution, potassium permanganate solution, and heat as developing agents. The ^{1}H and ^{13}C NMR spectra were recorded at 500 and 125 MHz (Agilent) with tetramethylsilane as an internal standard. Chemical shifts are indicated in δ values (ppm) from internal reference peaks (TMS ^{1}H 0.00; $CDCl_3$ ^{1}H 7.26, ^{13}C 77.00; DMSO-*d6* ^{1}H 2.50, ^{13}C 39.51). Melting points (mp) are uncorrected. High-resolution mass spectra (HRMS) were recorded on a Waters Synapt G2 HDMS (Waters, UK) mass spectrometer with an electrospray source acquired positive and negative ion data over a mass range 50-2000 m/z units. Microwave reactions were carried out in a Biotage Initiator microwave system 2.0 (400W, operating at 2.45 GHz). HPLC purifications using C18 analytical (Gracesmart RP 18, 4.6 mm × 250 mm) column was performed with Scientific Systems Inc. instrumentation comprising of 4-Q Grad Pumps connected to diode array (UV-Vis Thermo Finnigan Spectra system UV6000LP Detector, Lab Alliance (New York, USA). The LC-MS spectra were recorded on a LC-20AD Shimadzu connected to Shimadzu LCMS-2010EV equipped with C18 analytical column (Reprospher 100 C18-DE, 5µm 250 x 4.6mm, Dr Maisch GmbH). UV/Vis spectra were recorded with a Hitachi 2001 UV/Vis spectrometer (quartz 1cm). Fluorescence spectra were obtained on a Hitachi F7000 fluorimeter equipped with a Hamamatsu red sensitive R928 photomultiplier tube (Measurements were performed on air equilibrated samples, quartz 1cm^3). For PDT experiments a Lumi Source lamp (PCI Biotech, Oslo, Norway), blue light (λ = 435 nm, 13 mW/cm^2) was used.

Synthetic procedures

Methyl 3,5-bis(4,4,5,5-tetramethyl-1,3,2-dioxaborolan-2-yl)benzoate, 6: $Pd(dppf)Cl_2$ (22 mg, 6 mol-%) and methyl 3,5-dibromobenzoate **5** (150 mg, 0.51 mmol) were placed in a dry screw-cap vessel with a septum. Then, dry toluene (2.6 mL) was added, and the mixture was degassed with argon (1 min). Dry triethylamine (0.6 mL) and 4,4,5,5-tetramethyl-1,3,2-dioxaborolane (0.25 mL, 1.53 mmol) were successively added to the mixture. The reaction was ultrasonicated (1-2 min) to affect solution. The vial was transferred to the microwave synthesizer and after pre-stirring 15 s, irradiated for 8 h at 140 ^{o}C using a power setting of "High". After cooling, the reaction vessel was uncapped and the mixture was filtered through Celite. The filtrate was

concentrated and the residue was purified by flash chromatography (eluent; hexane/ethyl acetate = 10/1) to obtain 87 mg of **6** (total yield= 45%). **6:** ^{1}H NMR (500 MHz, $CDCl_3$) δ 8.55 (s, 2H), 8.43 (s, 1H), 3.91 (s, 3H), 1.35 (s, 24H); ^{13}C NMR (126 MHz, $CDCl_3$) δ 167.2, 145.4, 138.6, 132.3, 128.9, 84.0, 51.9, 24.9; FT-IR (KBr): 2980, 2952, 2929, 1720, 1595, 1450, 1401, 1372, 1333, 1320, 1248, 1167, 1143, 988 cm^{-1}; ESI-MS, positive mode (M=$C_{20}H_{30}B_2O_6$): m/z 389 $[M+H]^+$.

Methyl 3,5-di(pyridin-2-yl)benzoate, S1: A mixture of 1,3-diboronic acid dipinacol ester derivative **6** (275 mg, 0,708 mmol) and 2-chloropyridine (0.13 mL, 1.417 mmol) were dissolved in 7.5 mL THF. Then, Na_2CO_3 (601 mg, 5.67 mmol) in H_2O (1.4 mL), PPh_3 (111 mg, 0.425 mmol) and $Pd(OAc)_2$ (32 mg, 0.142 mmol) were added and the mixture was degassed with argon. The mixture was heated at 85 °C overnight. Subsequently, after cooling to rt the product was extracted with dichloromethane. The organic layers were dried over Na_2SO_4, filtered and concentrated under vacuum. The residue was purified by flash chromatography (eluent; hexane/ethyl acetate = 5/1) to afford 130 mg of compound **S1** (yield = 63%). Characterization was in agreement with literature data [39]. **S1:** ^{1}H NMR (500 MHz, $CDCl_3$) δ 8.92 (t, *J* = 1.8 Hz, 1H), 8.78 – 8.73 (m, 2H), 8.72 (d, *J* = 1.7 Hz, 2H), 7.91 (d, *J* = 7.8 Hz, 2H), 7.81 (m, 2H), 7.29 (m, 2H), 3.99 (s, 3H); ^{13}C NMR (126 MHz, $CDCl_3$) δ 166.8, 156.1, 149.7, 140.3, 136.9, 131.3, 129.8, 128.4, 122.7, 120.8, 52.3.

[4-(Methoxycarbonyl)-2,6-bis(pyridin-2-yl)phenyl]platinum(II) chloride, S2: Methyl-3,5-di(2-pyridyl)benzoate **S1** (130 mg, 0.448 mmol) was dissolved in acetonitrile (15 mL) and a solution of $K_2[PtCl]_4$ (186 mg, 0.448 mmol) in water (5 mL) was added, giving a yellow-orange solution. The reaction mixture was heated at vigorous reflux for 3 days, and then allowed to cool, giving a yellow precipitate. The precipitate was separated, washed with water (4 x 5 mL), ethanol (4 x 5 mL), acetonitrile (4 x 5 mL), and diethylether (2x5 mL), and then dried under reduced pressure. The product was isolated in 90% yield (208 mg). Characterization was in agreement with literature data [39]. **S2:** ^{1}H NMR (500 MHz, DMSO-d_6) δ 9.17 (d, *J* = 5.0 Hz, 2H), 8.35 (m, 4H), 8.30 – 8.19 (m, 2H), 7.71-7.54 (m, 2H), 3.91 (s, 3H); ESI-MS, positive mode (M= $C_{18}H_{14}N_2NaO_3Pt$): m/z 524.95 $[M-Cl+OH+Na]^+$.

4-Carboxy-2,6-bis(pyridin-2-yl)phenyl]platinum(II) Chloride, 3: KOH (755 mg, 13.46 mmol) was dissolved in MeOH (3.5 mL) and then [4-(methoxycarbonyl)-2,6-bis(pyridin-2-yl)phenyl]platinum(II) chloride (70 mg, 0.135 mmol) was suspended in this solution. The suspension was stirred at 40 °C for 24 h. After that, a 4M HCl (6.7 mL, 26.92 mmol) solution was added to the mixture. The yellow precipitate was washed with water (3 x 15 mL) and MeOH (2 x 15 mL) and the solvents evaporated to dryness. A yellow solid was obtained in 83% yield (80 mg). Characterization was in agreement with literature data [40]. **3:** ^{1}H NMR (500 MHz, DMSO-d_6) δ 12.98 (s, 1H), 9.15 (d, *J* = 5.5 Hz, 2H), 8.30 (m, 4H), 8.27-8.18 (t, *J*= 7.5 Hz, 2H), 7.61 (t, *J*= 7.5 Hz, 2H); ^{13}C NMR (126 MHz, DMSO-d_6) δ 167.7, 166.8, 165.6, 151.2, 140.6, 140.5, 125.9, 125.8, 124.5, 120.9; ESI-MS, positive mode (M= $C_{17}H_{12}N_2NaO_3Pt$): m/z 510.65 $[M-Cl+OH+Na]^+$.

4-(2,5-dioxopyrrolidin-1-yl)carbonyl-2,6-bis(pyridin-2-yl)phenyl]platinum(II) chloride, S3: To a solution of **3** (0.06 mmol, 30 mg) in DMF (0.6 mL), EDCI (0.07 mmol, 12.5 mg) and NHS (0.07 mmol, 7.5 mg) were added. The reaction mixture was left stirring overnight. A yellow precipitate was formed. The yellow solid was washed with DMF (3 X 0.5 mL) and dried to give 28 mg of **S3** in 77% yield. **S3:** ^{1}H NMR (500 MHz, DMSO-d_6) δ 9.02 (d, *J* = 5.5 Hz, 2H), 8.32-8.18 (m, 6H), 7.58 (t, *J* = 6.4 Hz, 2H), 2.97 (s, 4H); ^{13}C NMR (126 MHz, DMSO-d_6) δ 170.5, 170.1, 164.7, 162.3, 151.2, 141.2, 140.5, 125.9, 124.9, 121.4, 118.8, 25.6; FT-IR (KBr): 2958, 2923, 1736, 1608, 1588, 1479, 1425, 1364, 1342, 1242, 1202, 1069, 1036, 1007, 862; ESI-MS, positive mode (M= $C_{21}H_{15}N_3NaO_5Pt$): m/z 607.75 $[M\text{-}Cl+OH+Na]^+$.

Conjugate 4: To a solution of cRGDyK (3.2 µmol, 2 mg) in dry DMF (0.8 mL), DIPEA was added (3.8 µmol, 0.7 µL), following the addition of the activated ester **S3** (1.6 µmol, 0.96 mg). The reaction was left stirring at room temperature for 48 h and monitored by LC-MS. The solvent was evaporated *in vacuo* and the product was purified by reverse-phase HPLC (linear gradient from 0 to 100% B in 32 min, flow rate: 1 mL/min, R_t = 18 min). After chromatography 1.72 mg of conjugate **4** were obtained in 98% yield. The purity of the conjugate was confirmed by LC-MS and mass spectrometry (linear gradient from 90% H_2O to 10% acetonitrile, HCOOH 0.1%, over 30 min, flow rate: 0.4 mL/min, R_t = 13.5 min). ESI-MS with chromatographic separation, positive mode: m/z calcd mass for $C_{48}H_{57}ClN_{13}O_9Pt^+$ $[M\text{-}Cl+2ACN+H]^+$= 1189.37, was found 1189.56; calcd mass for $C_{44}H_{50}N_{11}O_9Pt^+$ $[M\text{-}Cl]^+$= 1071.35, was found 1071.15 calc mass for $C_{44}H_{52}N_{11}NaO_{10}Pt^{2+}$ $[M\text{-}Cl+H+CH_3CN]^{2+}$/2=556.68, was found 556.75; ESI-MS direct ionization, positive mode: m/z calcd mass for $C_{44}H_{51}ClN_{11}O_9Pt^+$ $[M+H]^+$=1107.32, was found 1107.95; calcd mass for $C_{44}H_{50}ClN_{11}NaO_9Pt^+$ $[M+Na]^+$=1129.3027, calcd mass for $C_{46}H_{54}ClN_{12}O_9Pt^+$ $[M+H+CH_3CN]^+$=1148.34 was found 1149.20; HRMS (ESI) with chromatographic separation m/z calcd for $C_{44}H_{51}N_{11}O_9Pt^+$ $[M\text{-}Cl]^{2+}$/2 =536.1756; was found 536.1739, $C_{46}H_{54}N_{12}O_9Pt^+$ $[M\text{-}Cl+H+CH_3CN]^{2+}$/2 =556.6890; was found 556.6889; ^{1}H NMR (500 MHz, DMSO-d_6 with 20 equiv NaCl) δ 9.16 (s, 1H), 9.15 (s, 1H), 8.63 (t, *J* = 5.3 Hz, 1H), 8.35 (s, 1H), 8.34 (s, 1H), 8.31 – 8.18 (m, 8H), 7.94 (d, *J* = 7.7 Hz, 1H), 7.61 (m, 3H), 6.89 (d, *J* = 8.2 Hz, 1H), 6.59 (d, *J* = 8.2 Hz, 1H), 6.52 (s, 1H), 4.67 (m, 1H), 4.43 (d, *J* = 14.0, 7.2 Hz, 1H), 4.22 (m, 1H), 4.10 (m, 2H), 3.09 (m, 2H), 2.87 (m, 1H), 2.83 – 2.70 (m, 1H), 2.64 (m, 2H), 2.41 – 2.32 (m, 2H), 2.08 (d, *J* =6.0 Hz, 1H), 2.00 (m, 1H), 1.75 (m, 1H), 1.65 (m, 1H), 1.52 (m, 2H), 1.40 (m, 1H), 1.25 – 1.16 (m, 4H) (1 proton is missing due to overlapping to DMSO-d_6); ^{13}C NMR (126 MHz, DMSO-d_6) δ 172.2, 171.7, 171.2, 170.9, 169.9, 169.5, 165.2, 156.6, 155.7, 150.6, 141.5, 141.3, 140.6, 129.9, 127.2, 124.9, 124.6, 123.8, 120.9, 114.9, 54.6, 51.9, 48.9, 43.2, 36.7, 34.9, 30.7, 29.1, 29.0, 28.7, 28.5, 26.6, 25.2, 22.8, 22.1 (2 carbons are missing due to overlapping to DMSO-d_6).

Spectroscopic characterization and singlet oxygen production of complex 3 and conjugate 4: UV quartz cuvettes with 1 cm path length were used. DMSO and THF were used as solvents with Teflon caps allowing flushing with Argon gas to remove oxygen from the solvent. Absorbance spectra were obtained using a U-

3010 spectrophotometer (Hitachi, Japan), and the software UV Solution. Steady state luminescence spectra were obtained using a Fluoromax II spectrometer.

The excited triplet state absorbance was measured using a NT 342B-SH-10-WW laser (Ekspla, Lithuania), array detector (Applied Photophysics, United Kingdom), and a Xenon flash lamp module (Model L9456-01, 5W, Hamamatsu) with BWSpec software (B&W Tek, USA). Transient absorption was obtained by firing the excitation OPO laser and flashlamp using DG535 Delay/Pulse generator (Stanford Research Systems) for control of triggers and detectors. Prior to measurement the sample was flushed with Ar-gas for 10 minutes in order to remove oxygen that quench the triplet signal. The recorded spectra was background corrected by subtracting the spectrum of pure solvent. Since the fluorescence was negligible, no need for fluorescence emission was needed. For details of the set-up and the procedure of analyzing similar triplet state absorption data, see Glimsdal et al [42].

The singlet oxygen production was demonstrated as the transient singlet oxygen luminescence (1275 nm) of a solution with the sample in a standard 90^{o} configuration. A tunable OPO laser, NT 342A-SH-10-WW (Ekspla, Lithuania) was used for excitation. For transient recording a PMT (R5509, Hamamatsu) and wavelength selective filters (interference filter with maximum transmission at 1272.5 nm and a long pass filter transmitting above 780 nm) were used, an Infiniium BDSU Oscilloscope (Keysight, United States) was used to collect data. A DG535 Delay/Pulse generator (Stanford Research Systems) was used to control the time between the laser excitation and the recording of the luminescence transient. The transients were background corrected by subtracting with signal of the same sample flushed with Argon for 10 min. A similar procedure for confirming singlet oxygen production of Ruthenium complexes for PDT was recently presented in Bogoeva et al [58].

Stability Evaluation: Aqueous stability of the conjugate was determined at pH 7.4 and 5.2. Conjugate **4** (0.32 mg, 0.289 µmol) was diluted in 30 µL DMSO and 16 µL solution of MeOH/H_2O (1/1). Next, 250 µL of buffer solution (phosphate buffer pH 7.4 or acetate buffer pH 5.2) was added and the solution was incubated at 37 °C. Mass spectra were recorded after 1, 3, 6, 24, and 48 h of incubation at 37 °C.

Reactivity toward aminoacids: Conjugate **4** (0.33 mg, 1.007 µmol) was diluted in 30 µL DMSO and 16 µL mixture of aminoacids L-histidine (1.007 µmol)/L-cysteine (1.007 µmol)/glycine (1.007 µmol) in MeOH/H_2O (1/1). Next, 250 µL of double distilled water was added and the solution was incubated at 37 °C. Mass spectra were recorded after 1, 3, 6, 24, and 48 h of incubation at 37 °C.

Cell lines: Three compounds conjugate **4**, compound **3** and c(RGDyK) were tested for anticancer activity against six well established human cancer cell lines (1 ovarian, 1 breast, 1 prostate cancer, 1 lung and 2 glioblastoma). SKOV-3 ovarian cancer cells, MCF7 breast adenocarcinoma cells, PC-3 prostate

adenocarcinoma cells, A549 lung adenocarcinoma cells, U251M and U87M, astrocytoma cells were tested for cytostatic (growth inhibition: IC_{50}, TGI) and cytotoxic/cytocidal (IC_{50}) activity against the three compounds at concentrations of 1-100 µM. The cell lines were obtained from the American Type of Culture collection (ATCC) and were grown in different culture medium according to the instructions. Cultures were maintained at 37 ^{o}C in 5% CO_2 and 95% air. Rat bladder transitional carcinoma cells (AY27) were maintained using RPMI-1640 culture medium (BioWhittaker) supplemented with 5% L-glutamine, 1% penicillin/streptomycin, 0.1% fungizone and 10% fetal bovine serum (FBS) in a humidified atmosphere of 37 ^{o}C in 5% CO_2 and 95% air as described in our earlier study [59].

Photodynamic Treatment*:* A number of 0.5 x 10^6 cells were seeded per Petri dish (diameter: 6 cm) and cultured for one day. Subsequent to wash cells with PBS twice, RPMI-1640 culture medium (FBS-free) containing different concentrations of the **3** or **4**, was added to cells and kept in the dark for 3.5 h. The medium was then replaced with PBS, and the cells were exposed to blue light (435 nm, 13 mW/cm^2) at different intervals (Lumi Source, PCI Biotech AS, Norway), given a total light dose of 7.8 J/cm^2 on the cell level during a 10 min illumination period, see Bogoeva et al [58]. The light was detected near the bottom of the cell dish and before passing the dishes. Subsequent to 18 h incubation, the viability of cultured cells were determined by the MTT assay [60, 61].

Fluorescence assays: U87 glioma and HeLa cervical cancer cells were maintained in DMEM medium supplemented with 10% fetal bovine serum (FBS) at 37 °C in 5% CO_2. For fluorescence assays, cells were cultured on coverslips overnight (24 well plate-7x10^4 cells per well) and the day after they were exposed to 10 µM of conjugate **4** and compound **3** for 0 and 2 h. To test the effect of the endocytosis inhibitor, okadaic acid, cells were preincubated, prior to addition of **4** and **3**, with medium containing DMSO (control) or okadaic acid (100 nM) for 30 min. Cells were then washed twice with PBS to remove floating conjugate and visualized in a Nikon confocal microscope using the EZ-C1 3.20 software.

MTT Assay: Cells were plated in 96-well plate at a density of 1x10^4cells/mL per well and maintained for 72 h at 37 ^{o}C in a 5% CO_2 incubator and grown as monolayers. After 24 hours, cells were treated with 0.1–100 µmol/L of the compounds for 48 h. The viability of cultured cells was estimated by an (3-(4,5-imethylthiazol-2-yl)-2,5-diphenyltetrazolium bromide (MTT) metabolic assay as described previously [60,61].

MTT (Sigma, St Louis, Missouri, USA) was dissolved in PBS in a concentration of 5 mg/mL, filter sterilized, and stored at 4 ^{o}C. MTT (50 µL of stock solution) was added to each culture and incubated for 3 h at 37 ^{o}C to allow metabolization. Formazan crystals were solubilized by DMSO (100 µL). Absorbance of the converted dye was measured at a wavelength of 540 nm on ELISA reader (Versamax, Orleans, USA). The mean concentrations of each drug that generated 50% or total (100%) growth inhibition (GI_{50} and TGI, respectively)

as well as the drug concentrations that produced cytotoxicity against 50% of the cultured cells [(half maximal inhibitory concentration (IC_{50})] were calculated using the linear regression method [62].

Using seven absorbance measurements [time 24 h (Ct24), control growth 72 h (Ct72), and test growth in the presence of drug at five concentration levels (Tt72x)], the percentage of growth was calculated at each level of the drug concentrations. The percentage growth inhibition was calculated according to National Cancer Institute (NCI) as:

[(Tt72x)-(Ct24) / (Ct72)-(Ct24)] x 100 for concentrations for which Tt72x>Ct24 and

[(Tt72x)-(Ct24)/Ct24] x 100 for concentrations for which Tt72x<Ct24

GI_{50} was calculated from [(Tt72x)-(Ct24)/(Ct72)-(Ct24)] x 100=50,

TGI from [(Tt72x)-(Ct24)/(Ct72)-(Ct24)] x 100=0, and

IC_{50} from [(Tt72x)-(Ct24)/Ct24] x 100= 50

All the experiments were carried out in triplicate.

References

[1] D. Van Straten, Mashayekhi, V., de Bruijn, H. S., Oliveira, S., Robinson. D. J. Oncologic Photodynamic Therapy: Basic Principles, Current Clinical Status and Future Directions, Cancers (Basel), 9 (2017) pii: E19.

[2] K. Lu, C. He, W. Lin. Nanoscale Metal–Organic Framework for Highly Effective Photodynamic Therapy of Resistant Head and Neck Cancer. J. Am. Chem. Soc. 136 (2014) 16712-16715.

[3] X. Wang, J. Hu, P. Wang, S. Zhang, Y. Liu, W. Xiong, Q. Liu, Analysis of the In Vivo and In Vitro Effects of Photodynamic Therapy on Breast Cancer by Using a Sensitizer, Sinoporphyrin Sodium. Theranostics 5 (2015) 772-786.

[4] R. K. Horlings, J. B. Terra, M. J. Witjes, mTHPC mediated, systemic photodynamic therapy (PDT) for nonmelanoma skin cancers: Case and literature review, Lasers Surg. Med. 47 (2015) 779–787.

[5] Z. Huang, A review of progress in clinical photodynamic therapy, Technol Cancer Res Treat. *4* (2005) 283-293.

[6] J. P. Celli, B. Q. Spring, I. Rizvi, C.L. Evans, K. S. Samkoe, S. Verma, B. W. Pogue, T. Hasan, Imaging and photodynamic therapy: mechanisms, monitoring, and optimization, Chem. Rev. 110 (2010) 2795e838.

[7]S. A. Sibani, P. A. McCarron, A. D. Woolfson, R. F. Donnelly, Photosensitiser delivery for photodynamic therapy. Part 2: systemic carrier platforms, Expert Opin Drug Deliv. 5 (2008) 1241-1254.

[8] R. V. Chari, M. L. Miller, W. C. WiddisonAntibody-drug conjugates: an emerging concept in cancer therapy, Angew. Chem. Int. Ed, Engl. 53, (2014) 3796-3827.

[9] M. A. Firer, G. Gellerman, Targeted drug delivery for cancer therapy: the other side of antibodies, J Hematol Oncol. 5, (2012) 70.

[10] S. Katsamakas, T. Chatzisideri, S. Thysiadis, V. Sarli. RGD-mediated delivery of small-molecule drugs, Future Med Chem. 9(6), (2017) 579-604.

[11] A. Dal Corso, L. Pignataro, L. Belvisi, C. Gennari, αvβ3 Integrin-Targeted Peptide/Peptidomimetic-Drug Conjugates: In-Depth Analysis of the Linker Technology, Curr. Top. Med. Chem. 16, (2016) 314-329.

[12] M. Huo, Q. Zhu, Q. Wu, T. Yin, L. Wang, L. Yin, J. Zhou, Somatostatin receptor-mediated specific delivery of paclitaxel prodrugs for efficient cancer therapy, J. Pharm. Sci. 104, (2015) 2018-2028.

[13] A. Nagy, A. V. Schally, G. Halmos, P. Armatis, R. Z. Cai, V. Csernus, M. Kovács, M. Koppán, K. Szepesházi, Z. Kahán Proc. Natl. Acad. Sci. U S A. 95, (1998) 1794-1799.

[14] B. P. Pemmaraju, S. Malekar, H. K. Agarwal, R. K. Tiwari, D. Oh, G. F. Doncel, D. R. Worthen, K. Parang, Design, synthesis, antiviral activity, and pre-formulation development of poly-L-arginine-fatty acyl derivatives of nucleoside reverse transcriptase inhibitors, Nucleosides Nucleotides Nucleic Acids 34, (2015) 1-15.

[15] M. Soler, L. Feliu, M. Planas, X. Ribas, M. Costas, Peptide-mediated vectorization of metal complexes: conjugation strategies and biomedical applications, Dalton Trans 45(33) (2016) 12970-12982.

[16] F. Danhier, A. Le Breton, V. Préat, RGD-based strategies to target alpha(v) beta(3) integrin in cancer therapy and diagnosis, Mol Pharm. 9(11) (2012) 2961-2973.

[17] S. Mukhopadhyay, C. M. Barnés, A. Haskel, S. M. Short, K. R. Barnes, S. J. Lippard, Conjugated platinum(IV)-peptide complexes for targeting angiogenic tumor vasculature, Bioconjug Chem. 19(1) (2008) 39-49.

[18]W. Cai, X. Chen, Anti-angiogenic cancer therapy based on integrin alphavbeta3 antagonism, Anticancer Agents Med. Chem. 6 (2006) 407-428.

[19] Y. Yuan, R. T. Kwok, B. Z. Tang, B. Liu, Targeted theranostic platinum(IV) prodrug with a built-in aggregation-induced emission light-up apoptosis sensor for noninvasive early evaluation of its therapeutic responses in situ, J. Am. Chem. Soc. 136(6) (2014) 2546-2554.

[20] A. Massaguer, A. González-Cantó, E. Escribano, S. Barrabés, G. Artigas, V. Moreno, V. Marchán, Integrin-targeted delivery into cancer cells of a Pt(IV) pro-drug through conjugation to RGD-containing peptides, Dalton Trans. 44(1), (2015) 202-212.

[21] A. Gandioso, E. Shaili, A. Massaguer, G. Artigas, A. González-Cantó, J. A. Woods, P. J. Sadler, V. Marchán, An integrin-targeted photoactivatable Pt(IV) complex as a selective anticancer pro-drug: synthesis and photoactivation studies. Chem. Commun (Camb) 51(44) (2015) 9169-9172.

[22] K. Chen, X. Chen, Integrin targeted delivery of chemotherapeutics, Theranostics. 1 (2011) 189-200.

[23] W. B. Edwards, W. J. Akers, Y. Ye, P. P. Cheney, S. Bloch, B. Xu, R. Laforest, S. Achilefu, Mol Imaging. 8 (2009) 101-110.

[24] D. Fan, X. Zhang, L. Zhong, X. Liu, Y. Sun, H. Zhao, B. Jia, Z. Liu, Z. Zhu, J. Shi, F. Wang (68)Ga-labeled 3PRGD2 for dual PET and Cerenkov luminescence imaging of orthotopic human glioblastoma Bioconjug Chem. 26 (2015) 1054-1060.

[25]F. L. Thorp-Greenwood, R. G. Balasingham, M. P. Coogan, Organometallic complexes of transition metals in luminescent cell imaging applications J. Organometal. Chem. 714 (2012) 12-21.

[26] C. K. Koo, L. K. So, K. L. Wong, Y. M. Ho, Y. W. Lam, M. H. Lam, K. W. Cheah, C. C. Cheng, W. M. Kwok. A triphenylphosphonium-functionalised cyclometalated platinum(II) complex as a nucleolus-specific two-photon molecular dye, Chemistry 16 (2010) 3942-3950.

[27] S. W. 3rd Thomas, K. Venkatesan, P. Müller, T.M. Swager, Dark-field oxidative addition-based chemosensing: new bis-cyclometalated PtII complexes and phosphorescent detection of cyanogen halides J. Am. Chem. Soc. 128, (2006) 16641-16648.

[28] J. A. G. Williams, S. Develay, D. L. Rochester, L. Murphy, Optimising the luminescence of platinum(II) complexes and their application in organic light emitting devices (OLEDs). Coordination Chem. Rev. 252, (2008) 2596–2611.

[29] K. Feng, R. Y. Zhang, L. Z. Wu, B. Tu, M. L. Peng, L. P. Zhang, D. Zhao, C. H. Tung, Photooxidation of olefins under oxygen in platinum(II) complex-loaded mesoporous molecular sieves J. Am. Chem. Soc. 128 (2006) 14685-14690.

[30] R. W. Sun, D. L. Ma, E. L. Wong, C. M. Che, Some uses of transition metal complexes as anti-cancer and anti-HIV agents. Dalton Trans. 43, (2007) 4884-4892.

[31] E. Glimsdal, M. Carlsson, T. Kindhal, M. Lindgren, C. Lopes, Eliasson. Luminescence, Singlet Oxygen Production, and Optical Power Limiting of Some Diacetylide Platinum(II) Diphosphine Complexes, J Phys. Chem. A 114 (2010) 3431-3442.

[32] A. Bossi, A. F. Rausch, M. J. Leitl, R. Czerwieniec, M. T. Whited, P. I. Djurovich, H. Yersin, M. E. Thompson Photophysical properties of cyclometalated Pt(II) complexes: counterintuitive blue shift in emission with an expanded ligand π system, Inorg Chem. 52 (2013) 12403-12415.

[33] B. Rosenberg, L. Vancamp, J. E. Trosko, V. H. Mansour, Platinum compounds: a new class of potent antitumour agents, Nature 222 (1969) 385-386.

[34] T. Boulikas, A. Pantos, E. Bellis, P. Christofis, Designing platinum compounds in cancer: structures and mechanisms. Cancer Therapy 5 (2007) 537-583.

[35] A. Colombo, F. Fiorini, D. Septiadi, C. Dragonetti, F. Nisic, A. Valore, D. Roberto, M. Mauro, L. De Cola, Neutral N^C^N terdentate luminescent Pt(II) complexes: their synthesis, photophysical properties, and bio-imaging applications, Dalton Trans, 44 (2015) 8478-8487.

[36] E. Baggaley, S. W. Botchway, J. W. Haycock, H. Morris, I. V. Sazanovich, J. A. Gareth Williams, J. A. Weinstein, Long-lived metal complexes open up microsecond lifetime imaging microscopy under multiphoton excitation: from FLIM to PLIM and beyond. Chem. Sci. 5, (2014) 879-886.

[37] R. E. Doherty, I. V. Sazanovich, L. K. McKenzie, A. S. Stasheuski, R. Coyle, E. Baggaley, S. Bottomley, J. A. Weinstein, H. E. Bryant, Photodynamic killing of cancer cells by a Platinum(II) complex with cyclometallating ligand. Sci Rep. 6, (2016) 22668.

[38] T. Ishiyama, M. Murata, N. Miyaura, Palladium(0)-Catalyzed Cross-Coupling Reaction of Alkoxydiboron with Haloarenes: A Direct Procedure for Arylboronic Esters, J. Org. Chem. 60 (1995) 7508–7510.

[39] J. A. G., Williams, A. Beeby, E. S. Davies, J. A. Weinstein, Wilson C. An Alternative Route to Highly Luminescent Platinum(II) Complexes: Cyclometalation with NΛCΛN-Coordinating Dipyridylbenzene Ligands. Inorg. Chem. 42, (2003) 8609-8611.

[40] B. Wieczorek, B. Lemcke, H. P. Dijkstra, M. R. Egmond, R. J. M. Klein Gebbink, G. van Koten Site-Selective Ser-Hydrolase Labelling with a Luminescent Organometallic NCN–Platinum Complex, Eur. J. Inorg. Chem. 13 (2010) 1929-1938.

[41] X. Feifan, C. Pieter, V. B. Jan. Electrospray ionization mass spectrometry for the hydrolysis complexes of cisplatin: implications for the hydrolysis process of platinum complexes. J Mass Spectrom. 52(7) (2017) 434-441.

[42] E. Glimsdal, I. Dragland, M. Carlsson, B. Eliasson, T. B. Melø, M. Lindgren Triplet Excited States of Some Thiophene and Triazole Substituted Platinum(II) Acetylide Chromophores, J. Phys. Chem. A, 113 (14) (2009) 3311–3320.

[43] W. Cai, Y. Wu, K. Chen, Q. Cao, D.A. Tice, X. Chen, In vitro and in vivo characterization of 64Cu-labeled Abegrin, a humanized monoclonal antibody against integrin alpha v beta 3. Cancer Res. 66, (2006) 9673-9681

[44] M. H. Lee, J. Y. Kim, J. H. Han, S. Bhuniya, J. L. Sessler, C. Kang, J. S. Kim, Direct fluorescence monitoring of the delivery and cellular uptake of a cancer-targeted RGD peptide-appended naphthalimide theragnostic prodrug. J. Am. Chem. Soc. 134 (2012) 12668-12674.

[45] M. S. Maginnis, J. C. Forrest, S. A. Kopecky-Bromberg, S. K. Dickeson, S. A. Santoro, M. M. Zutter, G. R. Nemerow, J. M. Bergelson, T. S. Dermody, Beta1 integrin mediates internalization of mammalian reovirus. J. Virol. 80 (2006) 2760-2770.

[46] X. Zhang, Z., Xiong, Y. Wu, W. Cai, J. R. Tseng, S. S. Gambhir, X. Chen, Quantitative PET imaging of tumor integrin alphavbeta3 expression with 18F-FRGD2. J Nucl Med. 47 (2006) 113-121.

[47] K. A. Hinchliffe, R. F. Irvine, N. DivechaAggregation-dependent, integrin-mediated increases in cytoskeletally associated PtdInsP2 (4,5) levels in human platelets are controlled by translocation of PtdIns 4-P 5-kinase C to the cytoskeleton. EMBO J. *15* (1996) 6516−6524.

[48] M. Higashihara, K. Takahata, K. Kurokawa, M. Ikebe, The inhibitory effects of okadaic acid on platelet function, FEBS Lett. 307 (1992) 206−210.

[49] I. Holen, P.B. Gordon, P. E. Stromhaug, T. O. Berg, M. Fengsrud, A. Brech, N. Roos, T. Bergs, P. O. Seglen, Inhibition of asialoglycoprotein endocytosis and degradation in rat hepatocytes by protein phosphatase inhibitors Biochem. J. *311* (1995) 317−326.

[50] C. M. Witkowski, I. Rabinovitz, R. B. Nagle, K. S. Affinito, A. E. Cress, Characterization of integrin subunits, cellular adhesion and tumorgenicity of four human prostate cell lines, J. Cancer Res. Clin. Oncol. *119* (1993) 637-644.

[51] S. A. Cannistra, C. Ottensmeier, J. Niloff, B. Orta, J. DiCarlo, Expression and function of beta 1 and alpha v beta 3 integrins in ovarian cancer, Gynecol. Oncol. 58 (1995) 216-225.

[52] L. Guo, F. Zhang, Y. Cai, T. Liu, Expression profiling of integrins in lung cancer cells, Pathol. Res. Pract. 205 (2009) 847-853.

[53] R. Czarnomysy, A. Surażyński, B. Popławska, E. Rysiak, N. Pawłowska, A. Czajkowska, K. Bielawski, A. Bielawska, Synergistic action of cisplatin and echistatin in MDA-MB-231 breast cancer cells. Mol. Cell Biochem. 427 (2017)13-22.

[54] P. M. Kazmierczak, A. Todica, F. J. Gildehaus, H. Hirner-Eppeneder, M. Brendel, R. S. Eschbach, M. Hellmann, K. Nikolaou, M. F. Reiser, H. J. Wester, S. Kropf, A. Rominger, C. C. Cyran. 68Ga-TRAP-(RGD)3 Hybrid Imaging for the In Vivo Monitoring of αvß3-Integrin Expression as Biomarker of Anti-Angiogenic Therapy Effects in Experimental Breast Cancer. PLoS One. 11 (2016) e0168248.

[55] H. A. Kim, K. Nam, S. W. Kim, Tumor targeting RGD conjugated bio-reducible polymer for VEGF siRNA expressing plasmid delivery. Biomaterials. 35(26) (2014) 7543-7452.

[56] E. Delamarre, S. Taboubi, S. Mathieu, C. Berenguer, V. Rigot, J. C. Lissitzky, D. Figarella-Branger, L. Ouafik, J. Luis, Expression of integrin alpha6beta1 enhances tumorigenesis in glioma cells, Am. J. Pathol. 175 (2009) 844-855.

[57] E. L. Larsen, L. L. Randeberg, O. A. Gederaas, C. J. Arum, A. Hjelde, C. M. Zhao, D. Chen, H. E. Krokan, L. O. Svaasand, Monitoring of hexyl 5-aminolevulinate-induced photodynamic therapy in rat bladder cancer by optical spectroscopy. J Biomed Opt. *13* (2008) 044031.

[58] V. Bogoeva, M. Siksjø, K. G. Sæterbø, T. B. Melø, A. Bjørkøy, M. Lindgren, O. A. GederaasRuthenium porphyrin-induced photodamage in bladder cancer cells, Photodiagnosis Photodyn Ther. 14 (2016) 9-17.

[59] Y. Baglo, M. M. Sousa, G. Slupphaug, L. Hagen, S. Håvåg, L. Helander, K. A. Zub, H. E. Krokan, O. A. Gederaas, Photodynamic therapy with hexyl aminolevulinate induces carbonylation, posttranslational modifications and changed expression of proteins in cell survival and cell death pathways. Photochem Photobiol Sci. 10(7) (2011) 1137-1145.

[60] G. J. Finlay, W. R. Wilson, B. C. Baguley Comparison of in vitro activity of cytotoxic drugs towards human carcinoma and leukaemia cell lines, Eur. J. Cancer Clin. Oncol. 22 (1986) 655–662.

[61] D. T. Trafalis, C. Camoutsis, P. Karamanakos, A. Arvanitis, E. Tegou, N. Ziras et al. Preclinical evaluation of the homo-aza-steroid ester 13-beta-hydroxy-13alpha-amino-13,17-seco-5alpha-androstan-17-oic-13,17-lactam-p-bis(2-chloroethyl)amino phenoxy acetate for the treatment of malignant melanoma, J BUON. *8* (2007) 333–339.

[62] M. C. Alley, D. A. Scudiero, A. Monks, M. L. Hursey, M. J. Czerwinski, D. L. Fine, B. J Abbott, J. G. Mayo, R. H. Shoemaker, M. R. Boyd Feasibility of drug screening with panels of human tumor cell lines using a microculture tetrazolium assay, Cancer Res. 48 (1988) 589–601.